Titanium Nitride/Carbon Coatings on Graphite Fibers

Yin Liu,* David R. Treadwell,* Mike R. Kannisto, Brian L. Mueller, and Richard M. Laine*

**Department of Materials Science and Engineering and Department of Chemistry, University of Michigan,
Ann Arbor, Michigan   48109–2136**

Titanium nitride (TiN) coatings were applied to graphite-fiber tows by dip coating desized (900°C in nitrogen) fibers in hexane solutions containing 0.5, 1, or 2 equivalent wt% TiN as the precursor, $-[Ti(NMe_2)_x(\mu-NCHMe_2)_{4-2x}]_n-$. The precursor was characterized by thermogravimetric analysis (TGA), chemical analysis, and nuclear magnetic resonance. Bulk samples of precursor were heated to selected temperatures in argon. Based on microstructural and chemical analyses—900° and 1200°C— were selected for more-detailed studies predicated on fiber oxidation-resistance behavior. At 900°C, the bulk material exhibited a powder X-ray diffractometry (XRD) pattern consistent with microcrystalline TiN, although some free carbon remained. XRD analysis of the samples pyrolyzed to 1200°C indicated a higher degree of crystallinity and some carbon incorporation in the TiN lattice; e.g., a TiCN solid solution forms, as supported by chemical and TGA analyses. Fibers coated with precursor were heated at a rate of 10°C/min in argon to selected temperatures, followed by a hold for 1 h, and the resulting coatings were characterized by scanning electron microscopy, X-ray photoemission spectroscopy, and oxidation resistance at 700°C for 2 h in air. Coated fibers pyrolyzed to 900° and 1200°C were studied in detail. Fibers heat treated at 900°C exhibited better oxidation resistance than fibers pretreated at 1200°C, as determined by mass loss. Uncoated fiber tows fully oxidized after 80 min. The oxidation-resistance studies on fiber tows pretreated at 900°C and coated with 0.5, 1, and 2 equivalent wt% TiN indicated that the sample with a coating of 1 wt%, with thicknesses of 0.1–0.2 μm, was the most stable. The coatings of 0.5 equivalent wt% TiN were irregular, whereas the coatings of 2 equivalent wt% TiN exhibited process-related cracking, leading to poor oxidation resistance.

I.   Introduction

THE performance of fiber-reinforced (polymer-, metal-, and ceramic-matrix composites (PMCs, MMCs, and CMCs, respectively)[1,2] depends greatly on the interaction between the composite components at mutual interfaces.[3–5] Fiber coatings are commonly used to modify interfacial interactions to optimize a variety of properties.[5–10] In actual use, they are expected to be multifunctional; i.e., they can enhance composite mechanical properties and protect fibers from chemical reaction with the environment.

Graphite fibers, which offer high specific strengths at relatively low cost, are widely used to reinforce all types of composites.[6] Unfortunately, they oxidize readily at temperatures of >500°C, which restricts their use as reinforcing materials for MMCs and CMCs and increases the difficulty of composite fabrication.[7] They also can react with matrix materials in MMCs to form metal carbides (e.g., Al_4C_3 in aluminum matrices), which damages fiber integrity, the matrix, and the interface.[8] The development of diffusion barriers that eliminate chemical reactions between graphite fibers and the matrix or the processing environment, while also providing appropriate interfacial mechanical properties, could resolve these problems.

To date, coating materials including TiC, SiC, SiO_xC_y, BN, B_4C, Al_2O_3, and MgO have been explored as a means of controlling interfacial properties and passivating graphite-fiber surfaces.[4,5,9,10] The wide variety of coating materials studied and required in MMC and CMC fabrication is predicated on the widely differing adhesive properties and chemical reactivities of the composite matrix materials used. Many of these coatings are readily applied via chemical or physical vapor deposition (CVD or PVD, respectively); however, both approaches are equipment and energy intensive. Consequently, we and others are exploring the use of dip coating fiber tows with preceramic polymer solutions, followed by firing, as a low-cost, alternative approach to high-quality coatings. To date, we have examined the fabrication of SiO_xC_y and mullite coatings on graphite fibers.[4,5] Here, we describe efforts to develop precursor-derived non-oxide coatings, with the initial focus on TiN.

TiN coatings are quite hard (22–32 GPa), which makes them useful in cutting-tool applications.[11] TiN also bonds strongly to many metals—e.g., aluminum alloys and steels—and, thus, may be a good interfacial material in MMCs.[12] TiN is isomorphous with TiC, which has already found use as a carbon-fiber coating.[13] TiN exhibits high-temperature stability, with a melting point of 2930°C and good chemical stability,[14] and is used for diffusion barriers in electronics and superalloy applications.[15–17] In addition, a polymeric precursor to TiN is readily available (see below). Unfortunately, TiN is susceptible to oxidation,[14] although the oxidation products TiO_xN_y and TiO_2 also are potentially useful coating materials. All of these suggest that TiN coatings may be of benefit in passivating carbon fibers and providing good-to-excellent interfacial properties.

TiN coatings are commonly produced via PVD and CVD methods.[11,18] $Ti(NMe_2)_4$ (where Me is a methyl group) is frequently used as a CVD precursor and provides high-quality TiN coatings.[14] $TiCl_4$ also has been used as a CVD precursor to produce TiC coatings on graphite fibers and TiN coatings on boron fibers.[9,13] Although the resulting coatings perform well, as noted above, CVD is equipment and energy intensive and, therefore, expensive. Moreover, both methods are inconvenient for processing large quantitites of fiber tows.

In principle, simply dipping continuous-fiber tows in a precursor solution and then heating the fiber tows to decompose the precursor coating to produce a uniform, defect-free ceramic coating appears simple and straightforward. In practice, two difficulties are encountered: (i) removing the organic ligands so that carbon contamination is avoided is not always easy, and (ii) obtaining good wetting such that uniform coatings of desired thickness are obtained is often hard.[19] The work reported here targets the use of soluble titanium amide precursors for dip coating graphite-fiber tows to produce uniform and defect-free TiN coatings following pyrolysis, with controlled coating properties, especially improved oxidation resistance.

II. Experimental Procedure

Thornel P-55 carbon fibers (Amoco, Chicago, IL) were used for dip coating. The as-received fiber properties include a typical diameter of ~10 μm (with sizing), a specific gravity of 2.0 g/cm^3, a tensile modulus of 380 GPa, a tensile strength of 1.90 GPa, a strain to failure of 0.5%, and a coefficient of thermal expansion of -0.9×10^{-6} °C^{-1} (0°–100°C, longitudinal). Methyllithium (CH$_3$Li), in diethyl ether, as the lithium bromide complex (1.5M solution), and dimethylamine, Me$_2$NH, anhydrous (99+%), were purchased from Aldrich Chemical Co. (Milwaukee, WI). Titanium tetrachloride (TiCl$_4$, 99%) was purchased from Alfa Co. (Ward Hill, MA). Isopropylamine, Me$_2$CHNH$_2$ (99%), was purchased from Pfaltz and Bauer (Waterbury, CT) and dried over CaH$_2$ before use. Hexanes (85% n-hexane) and toluene (Mallinckrodt, St. Louis, MO) were distilled from the appropriate drying agents under N$_2$ and stored under N$_2$ prior to use. All manipulations of air- or water-sensitive materials were conducted in argon or N$_2$ atmospheres using standard schlenk or glove-box techniques.

(1) Synthesis and Characterization of the TiN Polymer Precursor

(A) TiN Precursor: Ti(NMe$_2$)$_4$ (8.9 g), synthesized by the method of Bradley,[20] was dissolved in 20 mL of toluene in a 100 mL schlenk flask fitted with an efficient reflux condenser and a stir bar. The flask was placed in an oil bath at 60°C ($\pm$2°C). Isopropylamine (4.24 mL) (49.8 mmol, density of 0.694 g/mL), was added (ratio of 1.25 mol:1 mol titanium). Small bubbles immediately emerged from the solution, and the solution color changed from yellow to dark orange. To facilitate removal of dimethylamine, a slow stream of argon was admitted through the flask side arm and removed at the top of the condenser. After 6 h, no further bubbling was observed, and the reaction was assumed to be complete. On the removal of solvent, 14.6 g of precursor were recovered. The yield of TiN precursor, based on the proposed formula Ti[NCH$_3$)$_2$]$_{1.25}$-[N(CHCH$_3$)$_2$]$_{1.25}$, was 80% of theory.

(B) Nuclear Magnetic Resonance: Nuclear magnetic resonance (NMR) spectra were obtained on a spectrometer (Model Aspect 3000, AM-360 NMR, Bruker Co., Germany) operated at 360 (^{1}H) or 90.6 (^{13}C) MHz using 30° pulse widths and relaxation delays of 1.0 (^{1}H) and 0.5 (^{13}C) s. TiN precursor samples (0.2 mL) were dried under vacuum, then dissolved in 0.5 mL of C$_6$D$_6$ (Cambridge Isotope Labs, Cambridge, MA) under argon (D is deuterium), and then transferred to 5 mm NMR tubes. All chemical shifts are reported as parts per million (ppm) downfield of tetramethylsilane (TMS) (Aldrich).

(C) Thermal Analytical Techniques: Thermogravimetric analysis (TGA) studies were performed using a thermal analysis instrument (Model Hi-Res TGA 2950, TA Instruments, New Castle, DE). The sample and a platinum sample pan were weighed in an argon glove box and then transported out and loaded in the TGA instrument in an N$_2$ environment. The TGA was ramped at 10°C/min to 1000°C at the "High-Res 4" setting, with a 40 cm^3/min N$_2$ balance flow and a 60 cm^3/min air purge flow. The ceramic yield (TiO$_2$) for the precursor was 22.02% at 1000°C in air, corresponding to a TiN yield of 17.06%. The oxidation-resistance studies also were conducted by TGA, as discussed in the following section.

(2) Pyrolyses and Characterization of the Bulk Precursor

(A) Bulk Precursor Pyrolysis Studies: A typical experiment consisted of the following steps: (i) pumping a sample of precursor under dynamic vacuum for 3 h to remove traces of solvent and generate a viscous, red oil; (ii) transferring the sample to an argon glove box; (iii) placing ~500 mg of precursor into an alumina boat; (iv) placing the boat into a quartz tube; (v) sealing the quartz tube with a ported glass cap for gas ingress and egress; and finally (vi) taking the tube out of the argon glove box and placing it in a tube furnace (Model No. 58114, Lindberg, Watertown, WI) equipped with a programmable temperature controller (Model 818P, Eurotherm, Northing,

U.K.). Samples were then heated at a rate of 10°C/min to temperatures in the 200°–1200°C range in 200°C increments with a dwell time of 2 h at temperature, with argon flow passing through the quartz tube. The argon was prepurified by passing it through a heated column (150°C) of copper oxide. Samples were then cooled to room temperature, and the boat was reweighed to profile the ceramic yield at each temperature.

(B) Chemical Analysis: The vacuum-dried sample and the pyrolyzed samples were submitted for CHN analysis (chemical analysis for elemental carbon, hydrogen, and nitrogen). CHN analysis was conducted using an elemental analyzer (Model 2400 CHN, Perkin-Elmer, Norwalk, CT). The combustion tube was maintained at 1000°C with oxygen as the combustion gas, whereas the reduction tube was maintained at 640°C using helium as the carrier gas. The systematic error in measurements was $\pm$0.4 wt%.

(C) XRD Studies: Powder X-ray diffractometry (XRD) patterns were taken using a rotating anode goniometer (Rigaku Denki Co. Ltd., Tokyo, Japan). Pyrolyzed samples were ground in air using an alumina mortar and pestle. Then, the ground samples (40–80 mg) were loaded in a sample holder (glass plates) for data collection. The working voltage and current were 40 kV and 100 mA, respectively. Cu$K\alpha$ (λ = 1.54 A) radiation with a nickel filter was used. Scans were continuous from 5°–90° 2θ with a step scan of 10° 2θ/min and increments of 0.05° 2θ. The peak positions and the relative intensities of the pyrolyzed products were characterized by comparison with standard International Centre for Diffraction Data (ICDD, Newtowne Square, PA) files.

(3) Fiber-Coating Studies

(A) Coating Precursor Solutions: Precursor solutions of 0.5, 1, and 2 equivalent wt% TiN (200 g each) were made for fiber-coating studies. For example, a 200 g solution of 2 wt% TiN was made by mixing 177 g of hexane and 23.4 g of TiN precursor (TiN yield of 17.1 wt%), prepared as described above, together in a glass container inside an argon dry box. The glass containers were predried at 150°C for 24 h in air and transported while hot into the argon dry-box vacuum chamber.

(B) Fiber-Coating Procedures and Pyrolysis: Prior to coating, the sizing on the Thornel P-55 carbon fibers was removed as follows. Tows of carbon fibers, 60–80 cm in length, were wrapped lengthwise on a 20 cm $\times$ 5 cm $\times$ 0.6 cm graphite rack and placed inside a ported quartz tube. The quartz tube was placed in a Lindberg tube furnace and heated (in flowing argon) at 10°C/min to 900°C and held for 1 h to decompose the polymer sizing. The system was then allowed to furnace cool. Fibers were coated as follows.

For oxidation-resistance studies, the desized carbon-fiber tows were cut to lengths of 3–5 mm, placed into an argon glove box, and dipped in 0.5, 1, or 2 equivalent wt% TiN precursor solutions. After soaking for 2 min, the fibers were removed and allowed to dry for 15 min in the argon environment. The fibers were then placed in an alumina boat and loaded in the ported quartz tube again and heated (10°C/min/Ar) to selected temperatures (100 cm^3/min) and held at temperature for 1 h.

Longer fiber tows also were coated with the 1 or 2 equivalent wt% TiN solution. A rack containing the desized tows was dipped into the 1 or 2 equivalent wt% TiN solution, allowed to stand for 2 min, removed, and allowed to dry for 15 min in an argon environment. The dried fibers were heat treated in a manner identical to the cut fiber tows.

(C) Oxidation-Resistance Studies: Coatings were tested using TGA. Approximately 5 mg of fiber tow (3–5 mm in length, coated after cutting) were loaded in a platinum pan, heated at 50°C/min to 700°C, and held for 2 h in air (40 cm^3/min N$_2$ balance and 60 cm^3/min air purge flow).

(D) Scanning Electron Microscopy: The surface appearances of desized and coated carbon fibers were examined using a scanning electron microscopy (SEM) microscope (Model S800, Hitachi, Tokyo, Japan) operating at 5 keV. SEM samples were prepared by mounting carbon-fiber tows (3–5 mm in length) on an aluminum stub using carbon paste.

(E)   X-ray Photoelectron Spectroscopy: X-ray photoemission spectroscopy (XPS) spectra for bulk pyrolyzed powders and coated fibers were collected using an X-ray photoelectron spectrometer (Model 5400, PHI, Industry, CA). The powder XPS data were used as a reference for the fiber-coating analyses. A Mg X-ray source was operated at 300 W and 15 kV. The operating pressure was kept at $\sim$1.3 $\times$ 10^{-7} Pa ($\sim$10^{-9} torr) to minimize the signal from air. A small-area omni focus of 1 mm^2 was selected for sample analysis, and a neutralizer was used to prevent charge buildup.

Survey and multiplex analyses were conducted for each sample. Surveys were conducted over the 0–1000 eV energy range with an acquisition time of 5 min. The survey data provided basic information on peak positions for the elements found in the bulk powder and coating surfaces. Based on the survey information, multiplex analysis was performed for the interested energy ranges (or interested elements). The multiplex function gave a relatively accurate shape and position for the desired elemental peaks, from which the types of atomic bonding were evaluated, and permitted quantification of the surface compositions. Data were collected until the peaks of interest were visibly smooth (typically 1 h).

For all sample surfaces, the original surface was analyzed first, and then the surface following ion milling was analyzed. Surfaces were cleaned by argon-ion milling for >7 min for the powders and >2.5 min for the fibers, with a beam voltage of 3 kV. Milling rates were $\sim$10 A/min.

III.   Results and Discussion

### (1)   Precursor Synthesis and Characterization

The first goal in these studies was to develop an easily synthesized, rheologically useful, polymer precursor that transforms to dense, phase-pure TiN on pyrolysis. One other criterion requires that the precursor wet the substrate effectively to produce high-quality coatings. Based on previous efforts to synthesize non-oxide polymer precursors,[21] Ti(NMe$_2$)$_4$ was selected as the starting point for the synthesis of a processable TiN precursor.[14,19,20]

Because Ti(NMe$_2$)$_4$ is too volatile for fiber-coating purposes[20,22,23] and because methyl groups are likely to promote the formation of TiC,[24,25] a nonvolatile, soluble precursor with few methylamide moieties was sought.[26] Precursor solutions are potentially ideal for controlling coating thickness, because this can be done by simple adjustment of the precursor concentration, provided that good wetting can be obtained.

The TiN polymer precursor used in these studies was prepared by reacting Ti(NMe$_2$)$_4$ with 1.25 equiv of isopropylamine. The choice of 1.25 equiv was predicated on the need for a viscous polymer that coats well. Efforts to use >1.25 equiv resulted in highly crosslinked, intractable solids. The addition of isopropylamine, followed by heating, transformed yellow Ti(NMe$_2$)$_4$ hexane solutions to dark orange as dimethylamine was eliminated and the polymer formed:

Ti[N(CH$_3$)$_2$]$_4$ + 1.25(CH$_3$)$_2$CHNH$_2$ $\xrightarrow{60°C}$

Polymeric precursor + 2.5(CH$_3$)$_2$NH$\uparrow$ (1)
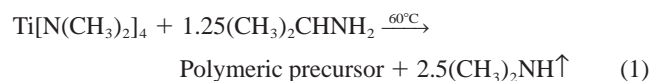
If reaction (1) proceeds as anticipated, the resulting polymer should be partially crosslinked with a structure similar to
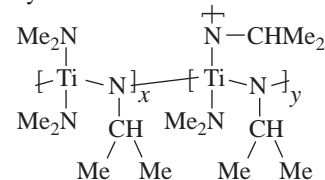
and with an empirical formula of C$_{6.75}$N$_{2.75}$H$_{17.75}$Ti. Dimeric (e.g. [(CH$_3$)$_2$N]$_2$Ti(NR)$_2$Ti[(CH$_3$)$_2$N]$_2$) and oligomeric species are known to form.[20] We believe that the product obtained here is polymeric, based on the initial reaction stoichiometry, NMR and CHN analyses, and the TGA ceramic yield at 1000°C (see below).

(A)   NMR Studies: NMR of the ^{13}C solution was used to establish a general solution structure. The ^{13}C values for Me$_2$NH, *i*PrNH$_2$, and Ti(N(CH$_3$)$_2$)$_4$, listed in Table I, provide resonances that support the proposed general molecular structure. For example, the carbon in free Me$_2$NH shifts from 36.8δ to 44.4δ (Δ = 7.6δ) when bound as an amido group in Ti(NMe$_2$)$_4$. The secondary carbon peak position of *i*PrNH$_2$ shifts from 43.3δ in the free amine to 61.3δ (Δ = 18.0δ) in the precursor complex. This much-larger shift likely results from an isopropylimido group bridging two titanium atoms rather than an amido complex.[20c] Proton NMR resonances (Table II) for the Me$_2$N and *i*PrN ligands shift as expected for terminal amides and bridging imides, respectively. Four distinct peaks are observed, suggesting a distribution of species, as expected for a partially crosslinked polymer. The dimer, if present, forms coincident with a number of oligomeric titanium species.

(B)   CHN Analysis: Chemical analysis of the vacuum-dried precursor gave the following values (in wt%): carbon, 43.1; hydrogen, 8.7; and nitrogen, 19.2 ($\pm$0.4 wt%). Values calculated for C$_{6.75}$N$_{2.75}$H$_{17.75}$Ti, corresponding to {Ti[NCH(CH$_3$)$_2$]$_{1.25}$[N(CH$_3$)$_2$]$_{1.5}$}, are as follows (in wt%): carbon, 43.8; hydrogen, 9.5; nitrogen, 20.8; and titanium, 25.9. These calculations assume a high polymer and do not include contributions from any remaining Me$_2$N– end groups. These values are relatively similar and, together with the NMR data, suggest that the proposed structure is reasonably accurate, as also supported by the TGA results below. The moisture sensitivity of the precursor precludes gel-permeation chromatographic molecular-weight analysis.

(C)   TGA Analysis: The TGA ceramic yield at 1000°C (at a rate of 10°C/min in air) for the vacuum-dried precursor is 43.23%. The off-white powder has been shown by XRD to be TiO$_2$. The theoretical TiO$_2$ yield, based on the proposed empirical formula, is 43.09%, which is within the error limits of the analysis method and again supports the proposed precursor structure.

(2)   Bulk Material Studies

The TiN precursor-to-ceramic transformation process, as a function of the pyrolysis temperature, was followed by mass-loss behavior and CHN, XPS, and XRD analyses to identify the various chemical and microstructural changes that occur. These

Table I. ^{13}C NMR Peak Positions for TiN Precursor

Chemical compound	^{13}C chemical shift† (δ)		
	C^1	C^2	C^3
HN(C^{3}H$_3$)$_2$			36.79
H$_2$NC^{1}H(C^{2}H$_3$)$_2$	26.69	43.27	
Ti(N(C^{3}H$_3$)$_2$)$_4$			44.38
Δδ of HN(C^{3}H$_3$)$_2$ on complexation with titanium			7.60
TiN polymer precursor	29.92	61.27	47.13, 47.65, 48.11
Δδ of HN(C^{3}H$_3$)$_2$ and H$_2$NC^{1}H(C^{2}H$_3$)$_2$ on complexation with titanium	3.23	18.00	10.34, 10.86, 11.32

†Spectra taken in benzene-d$_6$, using tetramethylsilane (TMS) as an internal standard. C^1 is the primary carbon in isopropylamine/isopropylimide, C^2 is the secondary carbon in isopropylamine/isopropylimide, and C^3 is the carbon is dimethylamine/dimethylamide.
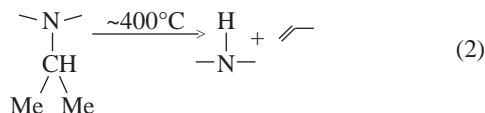
Table II. ¹H Peak Positions for TiN Precursor

	¹H chemical shift[†] (δ)		
Chemical compound	H¹	H²	H³
$HN(CH_3^3)_2$			2.18 singlet
$H_2NCH^1(CH_3^2)_2$	2.87 septet[‡]	0.92 doublet[‡]	
$Ti[N(CH_3^3)_2]_4$			3.10 singlet
Δδ of $HN(CH_3^3)_2$ on complexation with titanium			0.93
TiN polymer precursor	3.82, 4.36, 4.53 septet[‡]	1.21 doublet,[‡] 1.41, 1.47, 1.52	3.12 singlet, 3.18, 3.20, 3.26
Δδ of $HN(CH_3^3)_2$ and $H_2NCH^1(CH_3^2)_2$ on complexation with titanium	0.94, 1.49, 1.66	0.29, 0.49, 0.55, 0.60	0.94, 1.01, 1.02, 1.09

[†]H¹ is the primary hydrogen in isopropylamine/isopropylimide, H² is the secondary hydrogen in isopropylamine/isopropylimide, and H³ is the hydrogen in dimethylamine/dimethylamide. [‡]At J_{HH} 6.3 Hz.

studies were conducted to establish guidelines for processing and characterizing precursor-derived TiN coatings on graphite fibers.

(A) Pyrolysis Studies: We previously reported that the isobutyrate ligand (*i*PrCO₂) can be used as a general means of forming processable metal-oxide precursors.[27] These results prompted our efforts to use isopropylamine to form a processable TiN precursor. An additional motivation for choosing a secondary amine was the fact that the thermolysis of amine ligands with β-hydrogens frequently leads to direct cleavage of the C–N bond[28] rather than the metal–N bond, per reaction (2):

$$\overset{\diagdown}{N}\diagup \xrightarrow{\sim 400°C} \overset{H}{\underset{|}{N}} + \diagup\diagup \qquad (2)$$
$$\underset{\underset{Me\ \ Me}{\diagup\ \diagdown}}{\overset{|}{CH}}$$

Isopropyl rather than *n*-propyl groups were chosen to promote C–N bond cleavage, because the isopropyl moiety has six, rather than two, β-hydrogens and cleavage is more favorable if secondary carbon radicals form.[20c] The isopropyl groups would then most likely evolve as propene (reaction (2)),[24] generating hydrogenated TiN ($Ti_xN_yH_z$) first and then TiN on continued heating, because the residual hydrogen is lost as H_2 or CH_4, if any methyl groups remain. If pure TiN forms, then the theoretical ceramic yield would be 33.39%, based on an initial composition of $C_{6.75}N_{2.75}H_{17.75}Ti$.

The actual weight changes that occur when the dry precursor is pyrolyzed in 200°C increments from 200°C to 1200°C are shown in Fig. 1. On heating to 400°C, the polymerlike precursor transforms to a brittle material, suggesting extensive crosslinking and/or mineralization. The 50% mass loss at 400°C likely results from C–N bond cleavage, per reaction (2). On further heating to 800°C, an additional mass loss of 7% is observed,
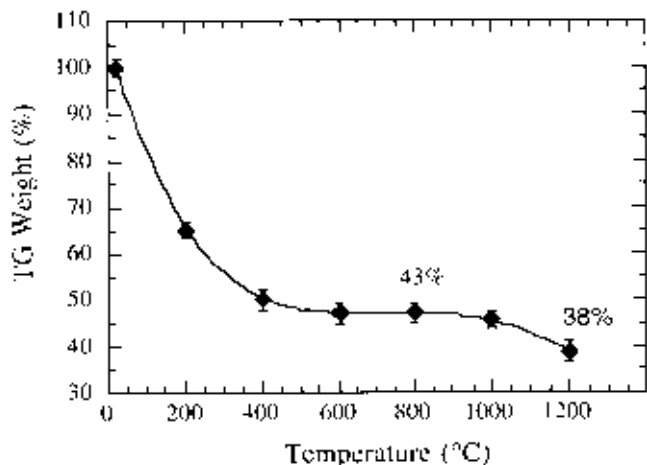
most of which appears to be nitrogen (see below). The mass losses at temperatures of >800°C also may result from the loss of nitrogen.

Chemical analysis indicates that the pyrolysis product is never pure TiN. The data in Fig. 1 show a 43% ceramic yield at 900°C, the pyrolysis temperature used for processing coated fibers. This value is 23 wt% higher than theory for pure TiN. In previous work, we observed that $Mo_2(NMe_2)_6$, on pyrolysis, converts to Mo_2C;[24] thus, the excess mass observed here is likely to be carbon that has been retained either as free carbon (graphitic or amorphous) or as the carbide, TiC.

In the samples pyrolyzed to 900°C, the carbon appears to be present as free carbon, based on TGA experiments (at a rate of 10°C/min in air to a temperature of 1000°C) involving samples prepyrolyzed to 900° or 1200°C. The samples prepyrolyzed to 900°C show a mass loss of 5 wt%. In contrast, pure TiN exhibits a 29% mass gain (also theory) when converted to TiO_2 under similar TGA conditions. These differences in mass gain/loss are accounted for if free carbon is present in the pyrolyzed material, because it will convert to CO or CO_2 on heating in air. From these mass-loss differences, the sample pyrolyzed to 900°C can be calculated to contain 25 wt% free carbon, which is similar to the values of 22 wt%, obtained by chemical analysis (see Fig. 2 and Table III), and 23 wt%, calculated from the Fig. 2 data, assuming the initial precursor composition is $C_{6.75}N_{2.75}H_{17.75}Ti$ and the sample transforms to pure TiN plus excess carbon.

The samples pyrolyzed to 1200°C exhibit a mass gain of 5 wt% on heating in air. If the mass-loss difference of 24 wt% (vs the anticipated 29 wt% gain) is a consequence of free carbon, these data correspond to 19 wt% free carbon present, which is less than the value of 25 wt% obtained by chemical analysis (see Fig. 2 and Table III). The XRD data presented below suggest that, at 1200°C, the remaining 5–6 wt% carbon is present as the carbide; i.e., TiCN has formed.

An additional argument for the presence of free carbon is that the alternative, based on the chemical analysis, would be the formation of mixtures of titanium carbide, titanium nitride, and carbon nitride. To date, true carbon nitride has not been synthesized.[29–34] Thus, we believe that the possibility of a C/N solid solution forming in the materials produced here is unlikely.

(B) Precursor Evolution as a Function of Pyrolysis Temperature (Chemistry): The chemical changes that occur as a function of pyrolysis temperature are discussed in terms of changes in elemental carbon, hydrogen, and nitrogen contents, as shown in Fig. 2. Hydrogen content changes in two stages. The major loss in hydrogen content occurs as the precursor transforms from a polymer to a ceramic char on heating to 550°C, with coincident loss of organics, e.g., propene or methane. Similar decreases in carbon content occur for the same reason. By 550°C, the hydrogen content decreases to <1 wt%. Note that 1 wt% hydrogen is the equivalent of 1 mol of hydrogen. Therefore, considerable hydrogen still remains, most likely as C–H and N–H bonds in the carbonaceous char. Elimination of this remaining hydrogen must occur through thermolytic
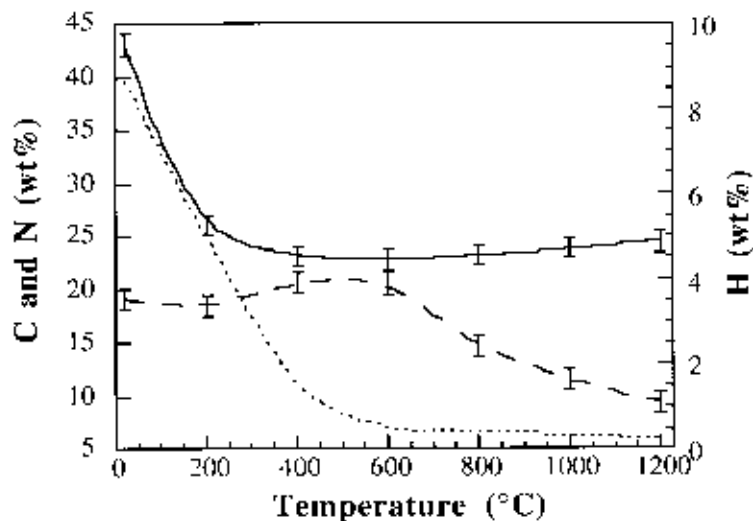

Fig. 1. Mass changes for TiN precursor pyrolyzed to selected temperatures for 2 h in argon.

Fig. 2. CHN chemical analysis ((—) carbon, (– –) hydrogen, and (--) nitrogen) showing compositional changes on pyrolysis to selected temperatures for 2 h in argon.

processes that cause hydrogen atoms to diffuse through the material until sufficient numbers of hydrogen atoms collect on the same carbon or nitrogen atom so that CH_4 or NH_3 evolve. Alternately, HCN or other simple carbon–nitrogen compounds can evolve.[34] Further loss of hydrogen is likely to be controlled by its diffusion rates in the char and will be slow until the highest pyrolysis temperatures are attained.

Carbon content also decreases on heating, until 550°C, as organic ligands are expelled, as discussed above. The carbon content at this stage is ~23 wt%. On heating to higher temperatures, carbon content increases slightly, mostly as a consequence of nitrogen loss. In contrast to the carbon content, but in keeping with the expected generation of propene[27] and methane, nitrogen content increases on heating to 550°C, from 19 wt% to 21 wt% (Fig. 2). The nitrogen content then decreases to 10% at 1200°C, most likely as a result of evolution of NH_3, HCN, or possibly N_2. As found in the XPS studies, the Ti:N ratio at 900°C is ~1:1. Thus, the considerable nitrogen loss on heating to 1200°C (Ti:N ratio = 2:1) may coincide with the formation of TiC or TiCN. Thus, fiber coatings pyrolyzed to 1200°C may convert to TiC or TiCN coatings.[25,26] This provides the rationale for contrasting fiber coatings processed at 900°C with those processed at 1200°C.

(C) XPS Data Analyses: Typically, XPS is used for the elemental analysis of surfaces. The XPS data for the pyrolyzed bulk precursor have been obtained to provide a reference for coating analyses (discussed in the following section). Table III presents XPS and chemical analyses for the precursor samples pyrolyzed to 900° and 1200°C.

Ion milling was used to clean the pyrolyzed precursor powder surfaces, to remove oxygen or other contaminants resulting from air exposure during XPS sample preparation. Ion milling removes ~10 A/min on a typical surface. However, because the XPS samples were pyrolyzed powders, rather than a simple plane surface, ion milling was prolonged and kept in a fixed direction to partially clean the powder surfaces. Some contribution from the original powder surfaces is likely to occur. Representative analyses of TiN and TiC surfaces from commercial powders are included in Tables III and IV for additional reference.

Because exposed surfaces adsorb oxygen during handling and sample preparation, the XPS data for the pyrolyzed bulk materials are not perfect. However, the data still suggest that the Ti:N ratio is ~1:1 at 900°C but increases to >2:1 for the sample pyrolyzed to 1200°C, as mentioned above.

Figure 3 shows the Ti $2p_{3/2}$ peaks for several samples. The Ti $2p_{3/2}$ peak positions for commercial TiC and TiN powders are shown in Fig. 3(A). Both samples contain adsorbed oxygen (as TiO_2) before ion milling, as indicated by the peak at 458.2 eV for TiC and 457.8 eV for TiN.[35] After ion milling, although the TiO_2 Ti $2p_{3/2}$ peak (~458 eV) still remains, the major Ti $2p_{3/2}$ peaks display TiC and TiN binding energies, both of which are 454.2 eV.

The Ti $2p_{3/2}$ peaks for the precursor pyrolyzed to 900°C are shown in Fig. 3(B). The bulk material, without ion milling, exhibits a TiO_2 peak at 458 eV.[35] After ion milling for 7 min, the Ti $2p_{3/2}$ peak shifts to a maximum at 454.2 eV. This suggests that the titanium that is present exists mainly as TiN (454.8 eV,

Table III.   XPS Data for Precursors Pyrolyzed to 900° and 1200°C and for a Commercial TiN

| Sample conditions | Amount (at.%) | | | | | Titanium:nitrogen ratio |
	Carbon	Oxygen	Titanium	Nitrogen	Hydrogen	
Pyrolyzed to 900°C	37	41	12	10		1.20
Pyrolyzed to 900°C, ion milled for 16 min	27	21	34	18		1.89
Pyrolyzed to 1200°C	61	23	11	5		2.20
Pyrolyzed to 1200°C, ion milled for 16 min	46	23	24	7		3.43
CHN chemical analyses for sample pyrolyzed to 900°C[†]	40.2 (22.3)		28.9 (64.2)	20.1 (13)	10.8 (0.5)	1.44
CHN chemical analyses for sample pyrolyzed to 1200°C[†]	47.1 (24.6)		31.5 (65.7[‡])	15.4 (9.4)	6.0 (0.3)	2.05
Commercial TiN	24	34	24	18		1.33
Commercial TiN, ion milled for 16 min		14	50	36		1.39

[†]Values in parentheses are the corresponding wt% values (±0.4%). [‡]Chemical analyses assume that carbon, hydrogen, nitrogen, and titanium are the only elements present in the precursor.

Table IV.   XPS Data for a Commercial TiC Powder

Sample	Amount (at.%)			Titanium:carbon ratio
	Carbon	Oxygen	Titanium	
Commercial TiC	34	43	23	0.68
Commercial TiC ion milled for 8 min	40	20	40	1

455.6 eV) or TiC (454.2 eV) but not as TiO_2 (458 eV).[35] The XRD data for the precursor pyrolyzed to 900°C discussed below also suggest that the material is crystalline TiN.

(D)   XRD Patterns: Figure 4(A) shows powder XRD patterns for precursors pyrolyzed to 400°, 900°, 1100°, and 1200°C with a dwell time of 1 h. All samples heated to temperatures of >400°C have been pyrolyzed at a rate of 2°C/min in argon to a temperature of 500°C and then at a rate of 10°C/min in argon to higher temperatures. The XRD data show peaks attributable to crystalline TiN (ICDD File Card No. 38-1420).

The broad peaks and poor intensities, as seen in the sample pyrolyzed to 400°C, suggest that considerable material is either amorphous or nanocrystalline. In Fig. 4(A), as the pyrolysis temperature increases, the XRD peak intensities increase and the peak widths decrease, indicating a greater degree of crystallinity and/or grain growth. Because TiC and TiN are almost isomorphous, the XRD peaks for the commercial powders can only be differentiated by careful examination of selected reflections (see below). Furthermore, the formation of a TiN/C solid solution would diminish the unit-cell parameter differences, which makes distinguishing between the two materials even more difficult. Thus, the formation of a TiN/C solid solution cannot be excluded based solely on XPS and XRD data. However, the ~1:1 Ti:N ratios found (by XPS and chemical analysis) at 900°C suggest mostly pure TiN with free carbon, unless some nitrogen is present as carbon nitride, which we find

unacceptable based on the carbon nitride literature.[34] Moreover, the TGA oxidation studies (see above) support our contention that at 900°C, the carbon is present as free carbon. A third argument comes from the TGA oxidation studies at 1200°C and the XRD analyses that follow.

Figure 4(A) also shows the XRD data for a commercial TiC powder, with peak positions corresponding to ICDD File Card No. 32-1383. Comparing the peak positions of the commercial TiN, the TiN precursor pyrolyzed to 900°C, and the commercial TiC powders, the TiC peaks are found at angles ~1° 2θ lower than those for TiN and for the maximum for the pyrolyzed samples. This is best illustrated using the Fig. 4(B) data for the (200) peak at 42.6° 2θ, suggesting that this material is TiN. However, Fig. 4(B) also shows that, at 1200°C, this peak shifts to 42.1° 2θ, which is closer to the (200) peak of TiC at 41.2° 2θ (ICDD File Card No. 32-1383, position 41.7° 2θ). Most likely, some carbon displaces nitrogen in the TiN lattice, shifting the unit-cell parameters closer to those of TiC at the higher pyrolysis temperatures. These results are in accord with our TGA oxidation findings that suggest ~6% of the 24.6% of carbon that is remaining at 1200°C is present as the carbide.

(3)   Coating Studies

As described above, graphite fibers were dip coated in TiN precursor solutions (0.5, 1, and 2 equivalent wt% TiN) and then pyrolyzed to selected temperatures in argon. These studies were
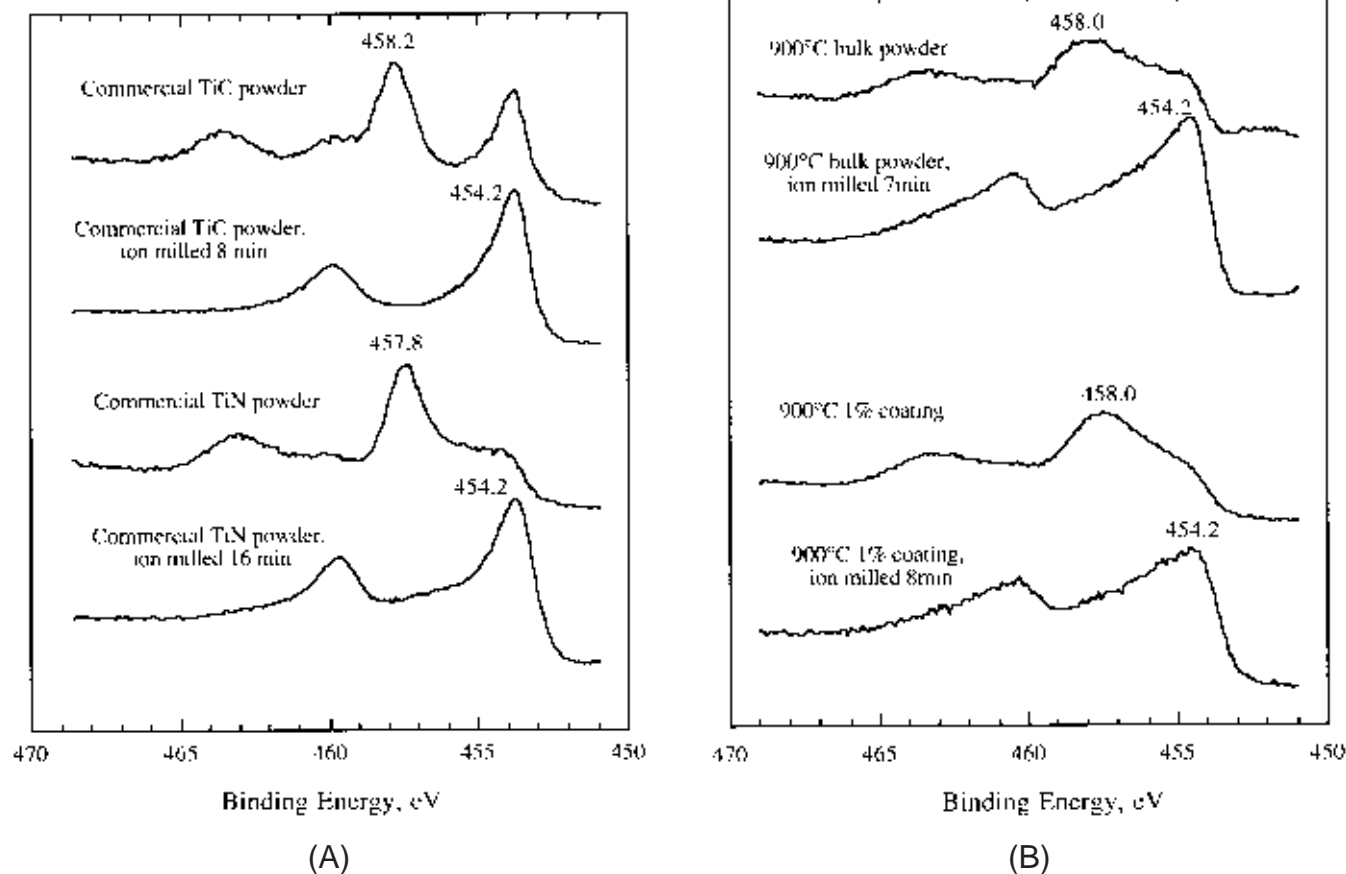

(A)

(B)

Fig. 3. XPS data for commercial powders: (A) pyrolyzed precursor, and (B) graphite fibers coated with 1 equivalent wt% TiN and pyrolyzed to 900°C for 1 h in argon.
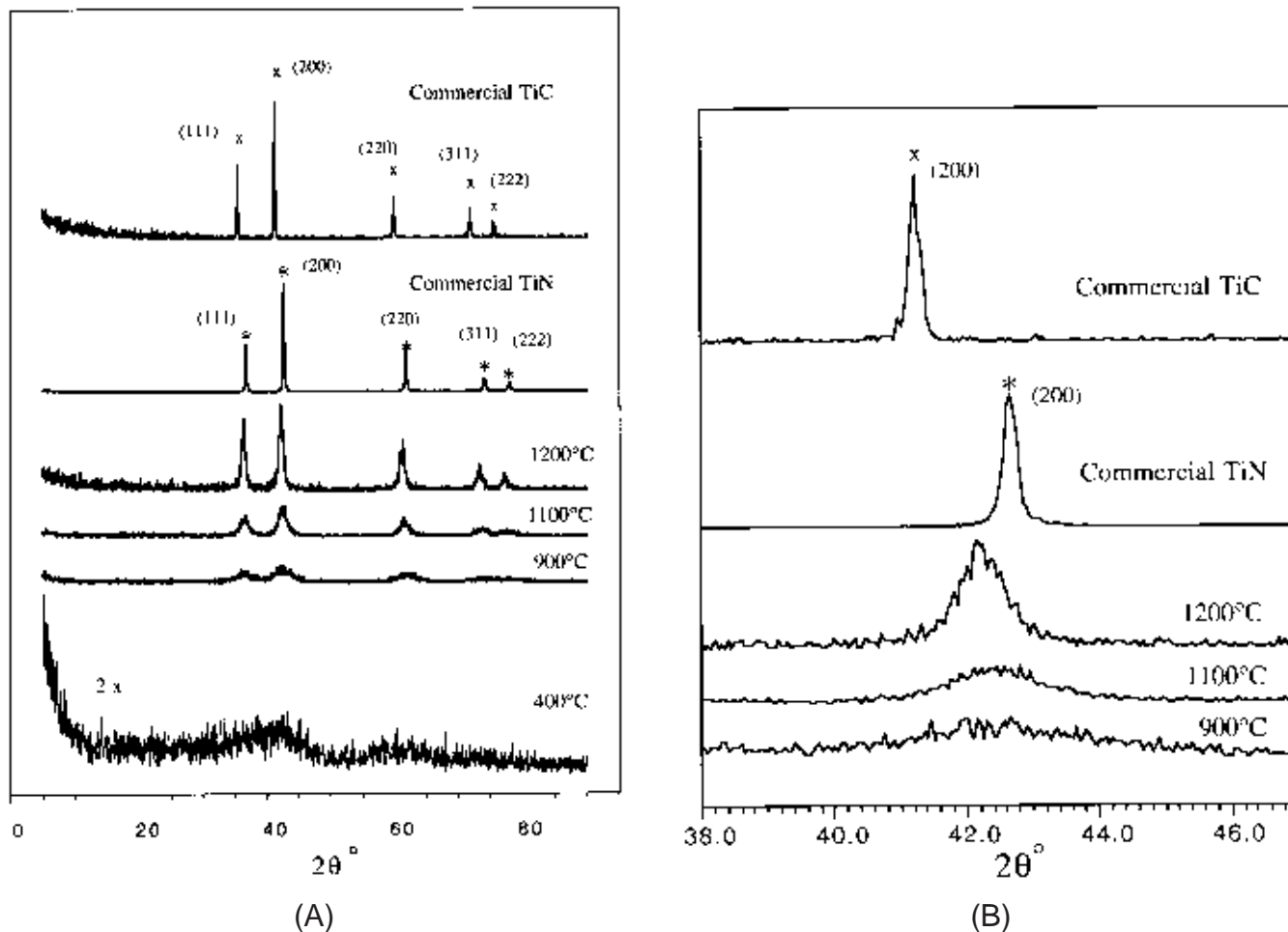
Fig. 4. (A) XRD for precursor solutions pyrolyzed to 400°, 900°, 1100°, and 1200°C, compared with the data for commercial TiN and TiC powders; (B) expanded view of the 38°–47° 2θ region shown in Fig. 4(A). Symbols "*" and "x" correspond to TiN (ICDD File Card No. 38-1420) and TiC (ICDD File Card No. 32-1383), respectively.

conducted to answer two questions. The first question is whether the coating solution can provide TiN coatings on graphite fibers. To address this question, XPS analyses of coated and pyrolyzed graphite fiber were conducted. The second question is what is the best processing route, including the concentration of the coating solution and the temperature of pyrolysis, to obtain the best coating properties. One important coating property is oxidation resistance. The oxidation-resistance properties for fibers processed via different routes were evaluated using TGA by holding the fibers at 700°C for 2 h in air. The coatings were evaluated by SEM to detect the presence of defects and to examine the microstructure and the thickness.

(A) Pyrolysis Temperature Studies: The bulk material studies suggest that microcrystalline TiN, contaminated with free carbon, is obtained at 900°C, based on the XPS and chemical analyses, which indicate a Ti:N ratio of ~1, almost the same as in pure TiN. At 1200°C, based on the bulk XPS and CHN results, the coating is more likely to be a TiCN coating, albeit somewhat more crystalline. To understand which coatings provide better oxidation resistance, the coatings pyrolyzed to 900° and 1200°C were compared.

(B) Graphite Fibers Coated with 1 equivalent wt% TiN Precursor and Pyrolyzed to 900°C in Argon: Figure 5 shows a micrograph of desized graphite fibers. The fiber diameter is 9±1 μm.[4] Cross sections of the fiber reveal striations associated with the orientation of the mesophasic pitch used to produce the fibers. After dip coating and pyrolysis, no visible changes in the fiber diameter are observed. Figure 6(A) shows a graphite fiber coated with a 1 equivalent wt% TiN precursor. At the lower right edge of the fresh-cut cross section, the debonded "skin"

indicates a coating thickness of 0.1–0.2 μm. Figure 6(B) provides a better view of the surface, which appears to be smooth and uniform; i.e., no cracks or pores are visible and the coating does not appear to debond from the surface. Hence, under these processing conditions, the polymer precursor coats fibers effectively and densifies uniformly on pyrolysis; the resulting ceramic coating wets the surface following pyrolysis.

XPS data for as-formed fiber coatings and for coated fibers that have been ion milled for 8 min are presented in Table V. The Ti:N ratio is 1.2:1 for the sample without ion milling and 1.6:1 for the sample that has been ion milled for 8 min. Commercial TiN gives values of 1.4:1, even after ion milling. Note that for the ion-milled bulk precursor, we observe a Ti:N value of 1:1, which is confirmed by chemical analysis. However, as noted above, XPS analyses of powders are assumed to be somewhat inexact. Consequently, these results, considered *in toto*, suggest that the coating consists primarily of TiN and carbon; quantification of the amounts of each is not possible. As with the bulk analyses, some oxygen also is observed and likely results from surface absorption, because the pyrolyzed fibers were handled in air. Figure 3(B) shows the Ti $2p_{3/2}$ binding-energy profiles for fresh surfaces with and without ion milling. These profiles appear to be very similar to the bulk precursor profiles. No changes in the peak positions are observed. Without ion milling, the binding energy observed is 458.0 eV, the same as the bulk sample data, and indicates the presence of TiO_2 on the coating surface. Recall that XPS analyses provide information to depths of 30–50 A only.[35] Similar to the behavior of the bulk precursor, after ion milling for 8 min, the Ti $2p_{3/2}$ peak position moves to 454.2 eV, which suggests the bonding is mainly TiN (454.8 eV, 455.6 eV), with carbon
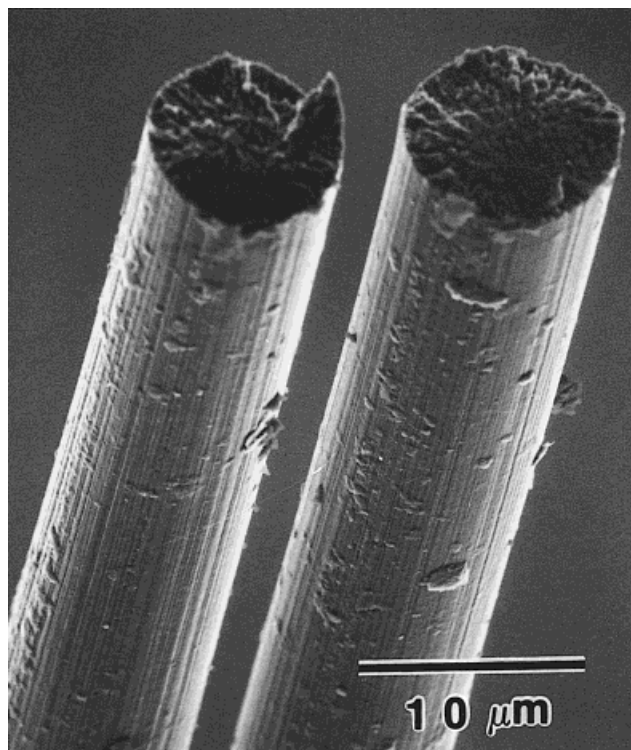
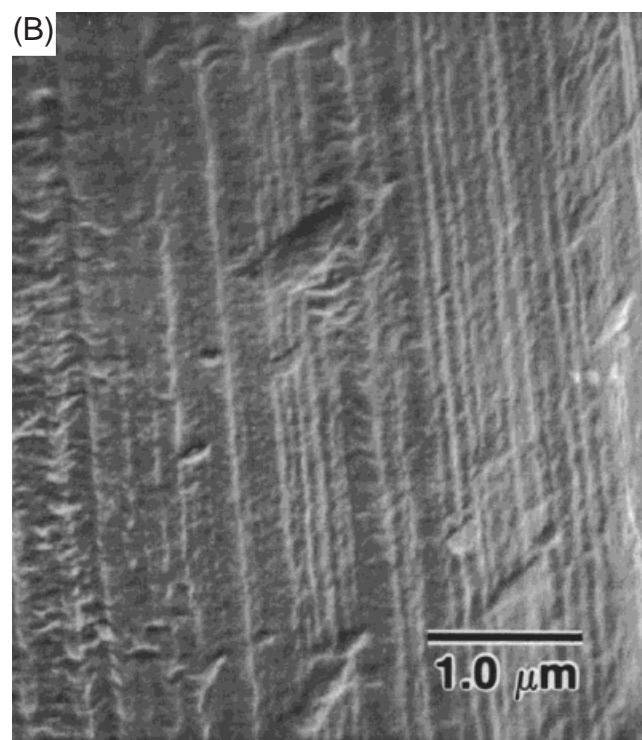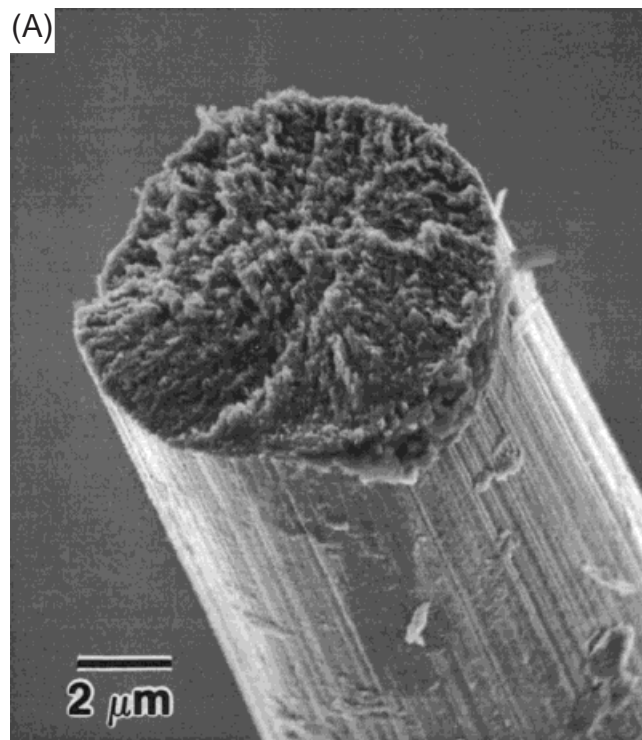**Fig. 5.** SEM micrograph of a graphite fiber desized by heating in argon to 900°C.

contamination.[35] Analyses of the coatings processed at 1200°C also are similar to the bulk studies.

(C)   Graphite Fibers Coated with 1 equivalent wt% TiN Precursor and Pyrolyzed to 1200°C in Argon: The higher degree of crystallinity obtained at 1200°C and the potential formation of TiCN rather than TiC coatings have prompted studies to ascertain whether improved coating properties could be obtained at 1200°C. Figure 7 shows an SEM micrograph of a graphite-fiber cross section coated with 1 equivalent wt% TiN, revealing a cracked (flawed) coating. Furthermore, the fiber surfaces exhibit a mottled texture, wherein the fiber striations are clearly visible between beads of material. A higher-magnification image (at 20000×; see Fig. 8) strongly suggests that dewetting has occurred. These beads are not observed for coatings pyrolyzed to 900°C (Fig. 6(B)). The XPS Ti $2p_{3/2}$ binding-energy profile for these surfaces (Fig. 3(B)) still exhibits peak maxima consistent with the presence of TiN/TiC or TiCN, although some TiO_2 is present on surfaces that have not been ion milled. One possible explanation for dewetting is that, at higher temperatures, crystallization, coupled with the alleviation of compressive stresses created during the initial precursor-to-ceramic transformation process, lead to grain growth with dewetting.

(D)   Oxidation Resistance of TiN-Coated Graphite Fibers Pyrolyzed to Different Temperatures: To establish the uniformity of the coatings and to develop a simple test of their reactivity, as measured by oxidation resistance, TGA oxidation studies were conducted using isothermal heating. Figure 9 shows that, on heating at a rate of 50°C/min in air to a temperature of 700°C, followed by an isothermal hold, uncoated fiber tows oxidize completely in 80 min. In contrast, fiber tows coated with 1 equivalent wt% TiN solutions and pyrolyzed to 900°C reproducibly retained ~55% of their initial weight at the end of the test (Fig. 9), indicating improved oxidation resistance. Fibers that were coated identically but heat treated to 1200°C exhibited lower oxidation resistance (Fig. 10). The inconsistent oxidation profiles that are shown suggest that coating integrity is lost at 1200°C, as expected from the SEM studies. Oxidation resistance similar to that of the fibers processed at 900°C was obtained in related studies with SiO_xC_y, mullite, and SiC coatings.[4,5,36]

(E)   TiN Solution Concentration Studies: Three different TiN solution concentrations—0.5, 1, and 2 equivalent wt%—


Fig. 6.   (A) SEM micrograph of a cross section of a graphite fiber coated with 1 equivalent wt% TiN and pyrolyzed to 900°C for 1 h in argon; (B) higher-magnification view of the area in Fig. 6(A).
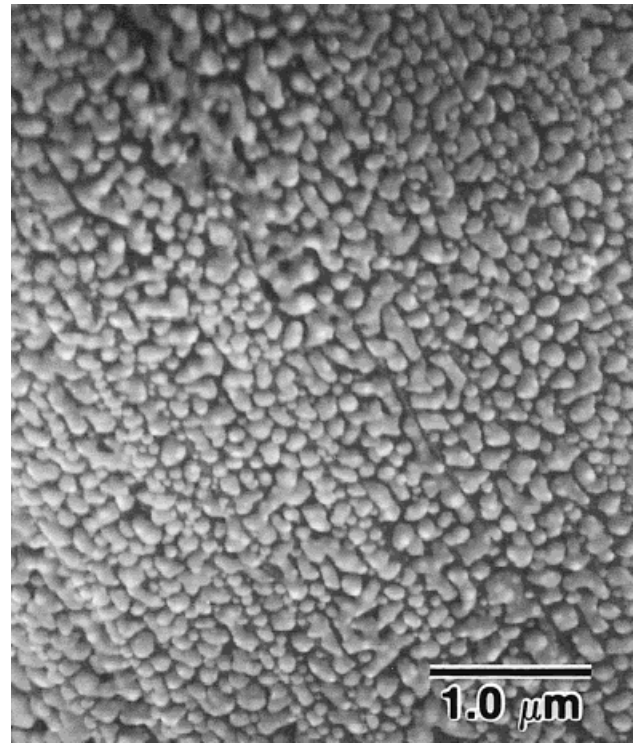
Table V. XPS Data for Graphite Fibers Coated with 1 Equivalent wt% TiN and Pyrolyzed to 900°C

XPS elemental analysis	Amount (at.%)				Titanium:nitrogen ratio
	Carbon	Oxygen	Titanium	Nitrogen	
Before ion milling	37.5	44.7	9.7	8.1	1.2
After ion milling for 8 min	84.7	7.1	5.0	3.2	1.6
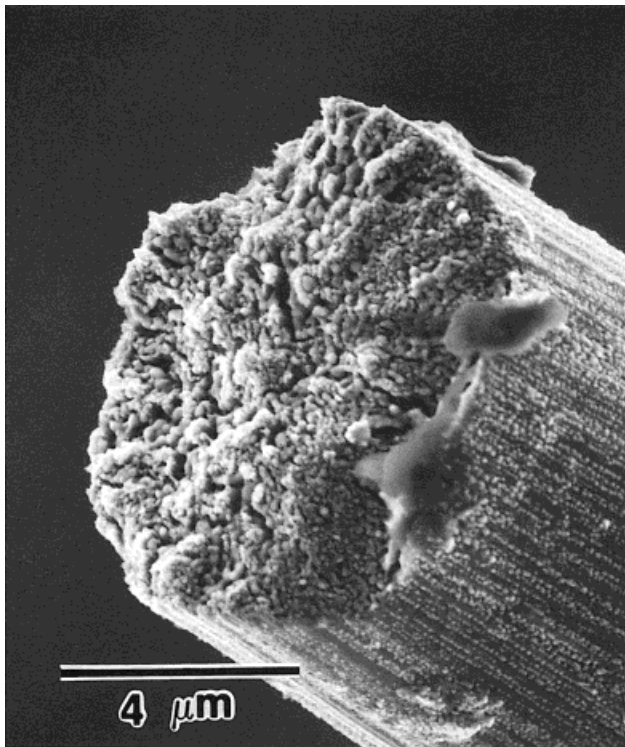
Fig. 7. SEM micrograph of a graphite fiber coated with 1 equivalent wt% TiN and pyrolyzed to 1200°C.

Fig. 8. SEM micrograph, at a magnification of 20000×, of a graphite fiber coated with 1 equivalent wt% TiN and pyrolyzed to 1200°C.
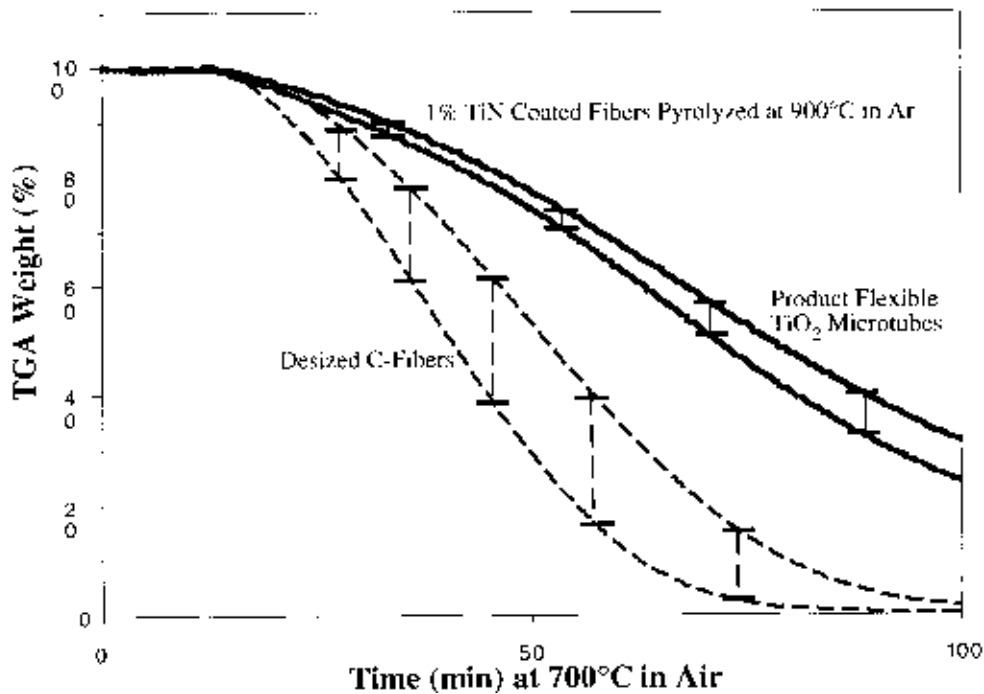
Fig. 9. TGA plots for graphite fibers coated with 1 equivalent wt% TiN (900°C) heated to 700°C in air.
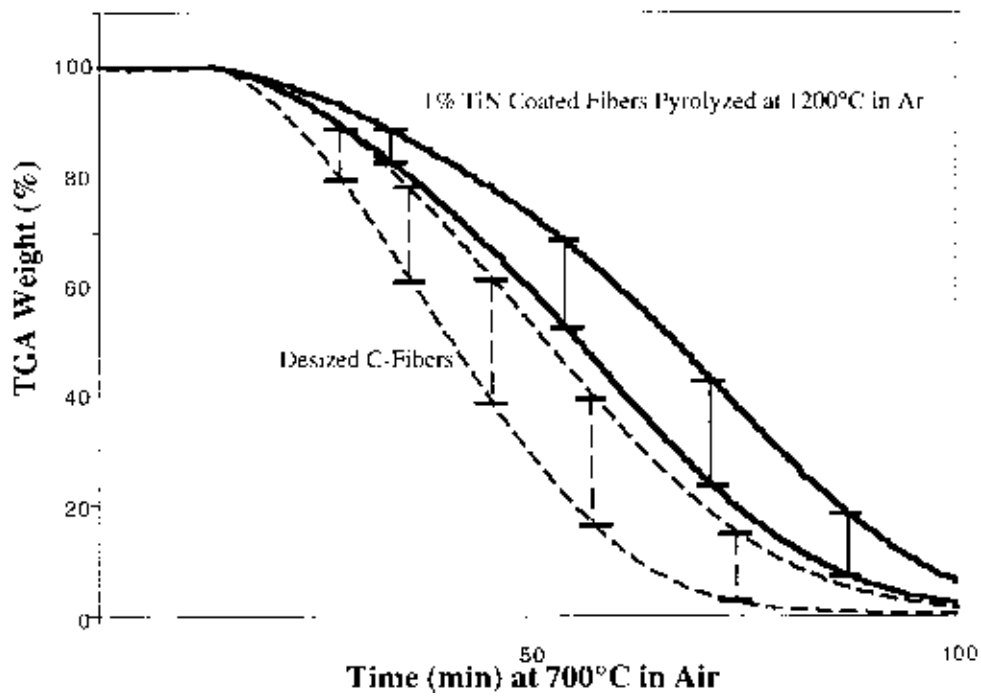
Fig. 10. TGA plots for graphite fibers coated with 1 equivalent wt% TiN (1200°C) heated to 700°C in air.

were studied. The coating properties were again evaluated by isothermal oxidation studies at 700°C for 3 h in air. Fiber tows coated with 0.5 equivalent wt% TiN and processed at 900°C exhibited erratic oxidation behavior (Fig. 11). Some tows behaved similarly to the uncoated ones and others retained >50% of their original mass at the end of the test (120 min), as observed for the tows coated with 1 equivalent wt% TiN. This behavior can be attributed to incomplete or insufficient coating of the fibers. The 2 equivalent wt% TiN coatings (pyrolyzed to 900°C for 1 h in argon) provided good, but erratic, oxidation resistance. In this instance, the average coating appears to have

been too thick (0.2–0.4 μm), leading to process-related cracking, as shown in Fig. 12. The cracks permitted the ingress of oxygen, leading to rapid oxidation.

The Fig. 9 TGA behavior of graphite-fiber tows coated with 1 equivalent wt% TiN (900°C) (shown in Fig. 9) must be treated as a lower limit for fiber-coating oxidation resistance, because some portion of the coated fiber ends crack during processing; the coatings at these ends are thicker than average (Fig. 13). For these fibers, oxidation starts from the fiber ends. Figure 14 shows the end of a graphite fiber coated with 1 equivalent wt% TiN and pyrolyzed to 900°C after heating at 650°C for 3 h in
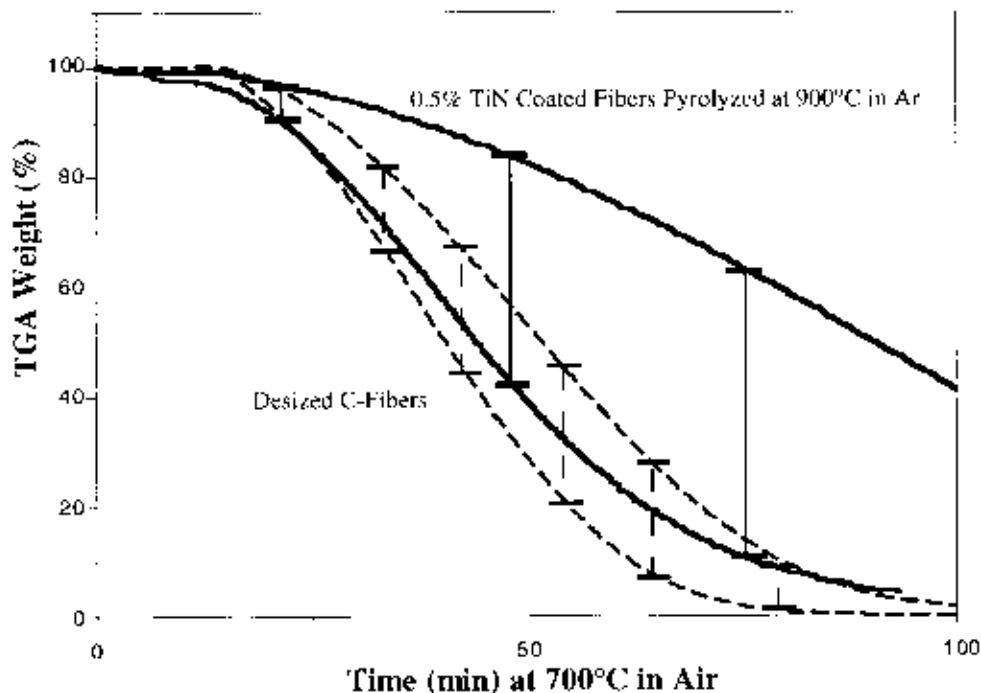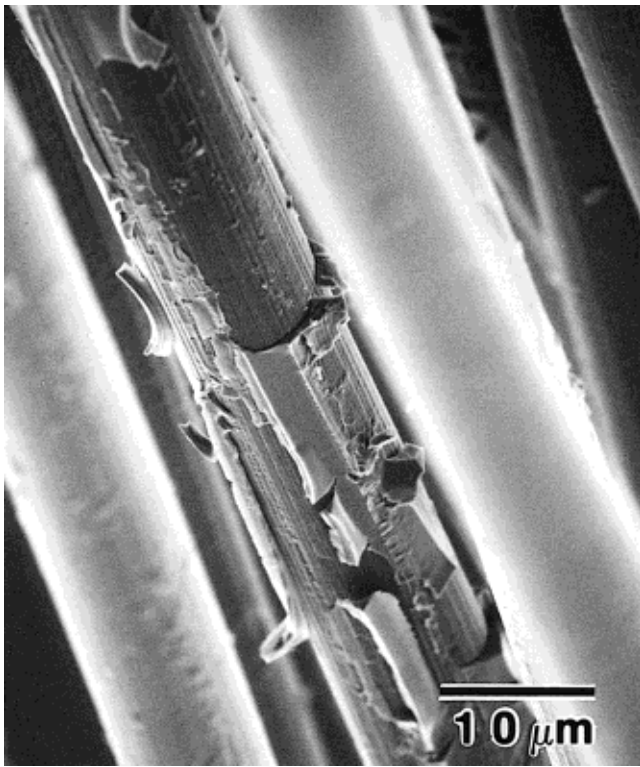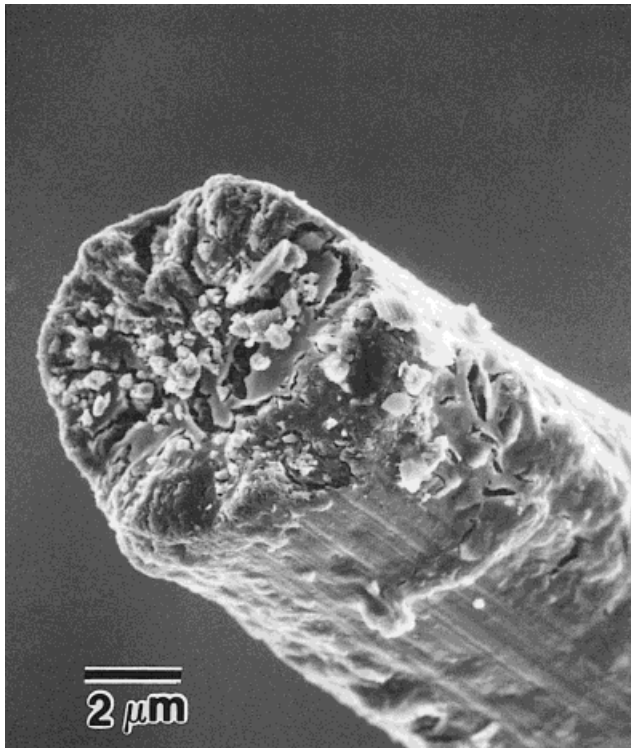

Fig. 11. TGA plots for graphite fibers coated with 0.5 equivalent wt% TiN (900°C) heated to 700°C in air.

Fig. 12. SEM micrograph of a graphite fiber coated with 2 equivalent wt% TiN and pyrolyzed to 1200°C for 1 h in argon.

Fig. 14. SEM micrograph of an end of a graphite fiber coated with 1 equivalent wt% TiN and pyrolyzed to 900°C that has been oxidized at 650°C for 3 h in air.

air. The hollow structure indicates that the graphite fiber oxidizes, leaving behind the skin of the ceramic coating. However, in the middle of the same fiber section, the graphite fiber remains unoxidized, indicating the actual oxidation resistance is likely higher than determined by TGA (Fig. 15).

IV. Summary

A processable, easily prepared TiN precursor, $[Ti(NMe_2)_x(NCHMe_2)_{4-2x}]_n$ was synthesized and then characterized by TGA, chemical analysis, and NMR. Based on these analyses, the general molecular structure is suggested to be
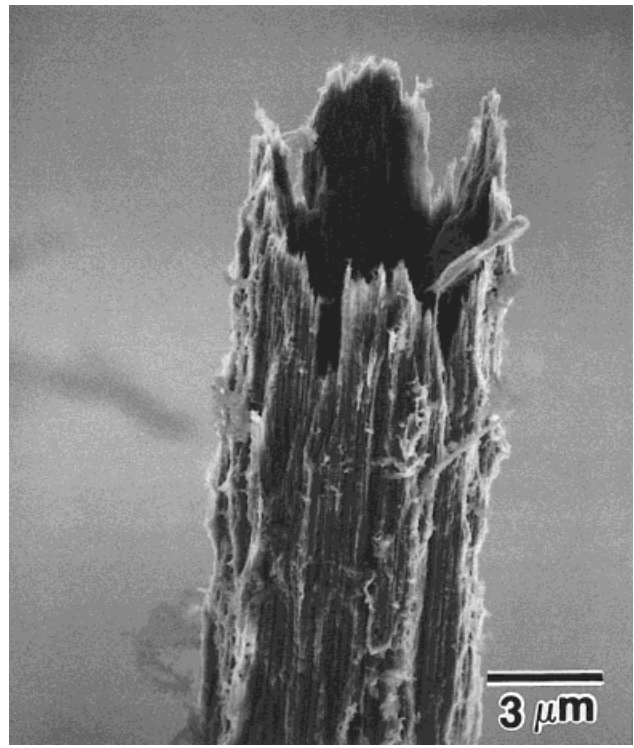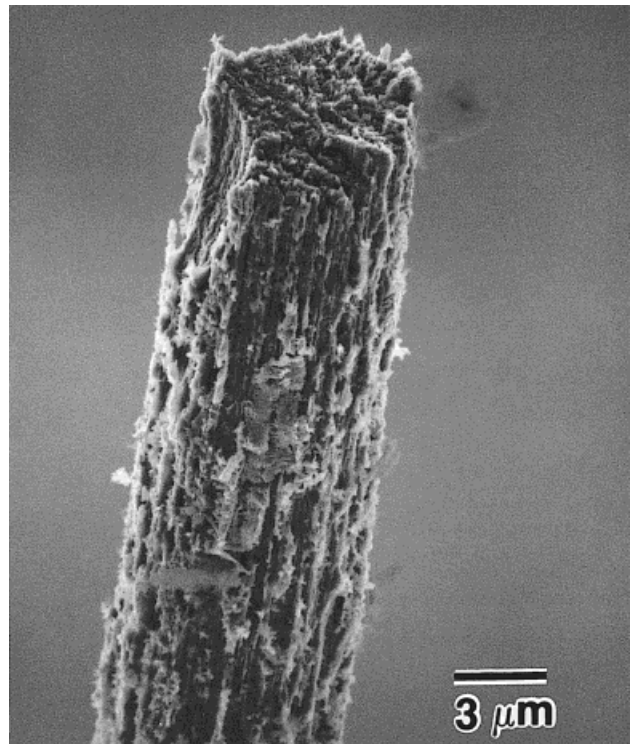

Fig. 13. SEM micrograph of a graphite fiber coated with 1 equivalent wt% TiN and pyrolyzed to 900°C for 1 h in argon.
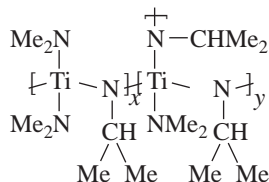

Fig. 15. SEM micrograph of the middle of a graphite fiber coated with 1 equivalent wt% TiN and pyrolyzed to 900°C that has been oxidized at 650°C for 3 h in air.

$$\begin{array}{c} Me_2N \qquad\qquad \overset{+}{N}-CHMe_2 \\ \left[\!\!\begin{array}{c} | \\ -Ti-N-Ti- \\ | \end{array}\!\!\right]_x \!\!-N\!\!-\right]_y \\ Me_2N \quad CH \quad NMe_2 \quad CH \\ /\backslash \qquad\qquad /\backslash \\ Me\ Me \qquad Me\ Me \end{array}$$

The phase and microstructural evolution that occurs on pyrolytic transformation of the precursor to a ceramic material has been followed by XRD, CHN, and XPS. On heating to temperatures of ≥900°C, a microcrystalline material is generated that is suggested by XPS and XRD to be primarily TiN. The Ti:N ratio at 900°C is ∼1:1; however, chemical analysis, TGA oxidation studies, and XPS indicate the presence of 22–24 wt% of free carbon. For material pyrolyzed to 1200°C for 1 h in argon, the Ti:N ratio is no longer 1:1, suggesting the formation of TiC and/or TiCN; the XRD data also suggest a powder pattern indicative of a TiN–TiC solid solution.

Three hexane precursor solutions were prepared, containing 0.5, 1, and 2 equivalent wt% TiN. Graphite fiber tows were dip coated in these solutions and pyrolyzed to 900°C for 1 h in argon or 1200°C for 1 h in argon (for 1 wt% TiN only). Coating composition and integrity were evaluated by XPS, SEM, and oxidation resistance. The best coatings were those obtained with the 1 equivalent wt% solutions and heated to 900°C, as determined by the relative absence of pores or cracks, with a thickness of 0.1–0.2 μm.

The oxidation resistance of the resulting ceramic coatings was compared by following the weight loss in TGA at 700°C over a period of 2 h. The TGA profiles demonstrated improved oxidation resistance after coating. The fiber tows coated with 1 equivalent wt% TiN retained >50% of their mass after 100 min, whereas the fiber tows coated with 0.5 and 2 equivalent wt% TiN exhibited erratic oxidation behavior, because of processing flaws. Uncoated fiber tows oxidized fully after 80 min.

References

[1]R. N. Singh, "Fiber–Matrix Interfacial Characteristics in a Fiber-Reinforced Ceramic-Matrix Composite," *J. Am. Ceram. Soc.*, **72** [9] 1764–67 (1989).

[2]R. N. Singh and M. Sutcu, "Determination of Fiber–Matrix Interfacial Properties in Ceramic-Matrix Composites by a Fiber Push-out Technique," *J. Mater. Sci.*, **26**, 2547–56 (1991).

[3](a) D. Hull, *An Introduction to Composite Materials*. Cambridge University Press, Cambridge, U.K., 1981. (b) A. G. Metcalfe and M. J. Klein, "Effect of the Interface on Longitudinal Tensile Properties"; pp. 125–68 in *Interfaces in Metal Matrix Composites, Composite Materials, Vol. 1*. Edited by A. G. Metcalfe. Academic Press, New York, 1974.

[4]M. Harris, T. Chaudhary, L. Drzal, and R. M. Laine, "Silicon Oxycarbide Coatings on Graphite Fibers: Chemistry, Processing, and Oxidation Resistance," *Mater. Sci. Eng. A*, **195**, 233–36 (1995).

[5]P. Kansal, "Mullite Coatings on Graphite Fibers: Precursor Synthesis, Processing, Characterization and Oxidation Resistance"; Ph.D. Dissertation. Department of Material Science and Engineering, University of Michigan, Ann Arbor, MI, 1996.

[6]A. P. Diwanji and I. W. Hall, "Fibre and Fibre-Surface Treatment Effects in Carbon/Aluminium Metal Matrix Composites," *J. Mater. Sci.*, **27**, 2093–100 (1992).

[7]P. Ehrburger and E. Dallies-Labourdetle, "Inhibition of the Oxidation of Carbon Fibres and Composites," *Tanso*, **155**, 359–64 (1992).

[8](a) H.-M. Cheng, B.-L. Zhou, A. Kitahara, S. Akiyama, and K. Kobayashi, "Effect of Silicon Additions on Characteristics of Carbon Fiber Reinforced Aluminum Composites During Thermal Exposure," *J. Mater. Res.*, **11** [5] 1284–92 (1996). (b) H.-M. Cheng, A. Kitahara, S. Akiyama, K. Kobayashi, Y. Uchiyama, and B.-L. Zhou, "Characteristics of Several Carbon Fibre-Reinforced Aluminium Composites Prepared by a Hybridization Method," *J. Mater. Sci.*, **29**, 4342–50 (1994).

[9]B. J. Tan, L. Hwan, S. L. Suib, and F. S. Galasso, "Chemical Vapor Deposition TiN Coating on Silicon Carbide Coated Boron Fibers," *J. Vac. Sci. Technol. A*, **9** [4] 2196–203 (1991).

[10](a) Y. Xie and P. M. A. Sherwood, "Coatings of Aluminum Oxide and Magnesium Oxide on Carbon Fiber Surfaces," *Chem. Mater.*, **6**, 650–57 (1994). (b) C. Vincent, H. Vincent, H. Mourichoux, and J. Bouix, "Characterization by XPS and SEM of Reactive Chemical Vapour Deposited Boron Carbide on Carbon Fibre," *J. Mater. Sci.*, **27**, 1892–900 (1992).

[11]W. C. Oliver, C. J. McHargue, and S. J. Zinkle, "Thin Film Characterization Using a Mechanical Properties Microprobe"; pp. 185–96 in *Metallurgical Coatings 1987, Vol. I*. Edited by R. C. Krutenat. Elsevier, New York, 1987.

[12]E. Erturk and H.-J. Heuvel, "Adhesion and Structure of TiN Arc Coatings," *Thin Solid Films*, **153**, 135–47 (1987).

[13]M. D. Sanctis, S. Pelletier, Y. Bienvenu, and H. Vincent, "Filamentary Preforms of Al–13 wt% Si Alloy Reinforced with TiC-Coated and Pre-treated Carbon Fibres," *J. Mater. Sci.*, **29**, 356–65 (1994).

[14]R. M. Fix, R. G. Gordon, and D. M. Hoffman, "Synthesis of Thin Films by Atmospheric Pressure Chemical Vapor Deposition Using Amido and Imido Titanium(IV) Compounds as Precursors," *Chem. Mater.*, **2**, 235–41 (1990).

[15](a) M.-A. Nicolet, "Diffusion Barriers in Thin Films," *Thin Solid Films*, **52**, 415–43 (1978). (b) M. Wittmer, B. Studer, and H. Melchior, "Electrical Characteristics of TiN Contacts to *N* Silicon," *J. Appl. Phys.*, **52** [9] 5722–26 (1981). (c) S. Kanamori, "Investigation of Reactively Sputtered TiN Films for Diffusion Barriers," *Thin Solid Films*, **136**, 195–214 (1986).

[16]C. Y. Ting, "TiN Formed by Evaporation as a Diffusion Barrier Between Al and Si," *J. Vac. Sci. Technol. B*, **21** [1] 14–18 (1982).

[17]J. R. Shapirrio, "Diffusion Barriers in Advanced Semiconductor Device Technology," *Solid State Technol.*, **28** [10] 161–66 (1985).

[18]L. H. Dubois, B. R. Zegarski, and G. S. Girolami, "Infrared Studies of the Surface and Gas Phase Reactions Leading to the Growth of Titanium Nitride Thin Films from Tetrakis (dimethylamido) Titanium and Ammonia," *J. Electrochem. Soc.*, **139** [12] 3603–609 (1992).

[19](a) C. Russel, "Preparation and Pyrolysis of a Polymeric Precursor for the Formation of TiN–TiC Solid Solutions," *Chem. Mater.*, **2**, 241–44 (1990). (b) D. Seyferth and G. Mignani, "Preparation of Titanium Nitride and Titanium Carbonitride by the Preceramic Polymer Route," *J. Mater. Sci. Lett.*, **7**, 487–88 (1988).

[20](a) D. C. Bradley and I. M. Thomas, "Metallo-organic Compounds Containing Metal–Nitrogen Bonds, Part I. Some Dialkylamino-Derivatives of Titanium and Zirconium," *J. Chem. Soc.*, 3857–61 (1960). (b) D. C. Bradley and E. G. Torrible, "Metallo-organic Compounds Containing Metal–Nitrogen Bonds, Part IV. Some Bis-(Primary Amino)-Titanium Compounds," *Can. J. Chem.*, **41**, 134–38 (1963). (c) C. T. Jekel-Vroegop and J. H. Teuben, "Monoalkyl and Nomoaryl–Amidotitanium Complexes," *J. Org. Chem.*, **286**, 309–15 (1985).

[21](a) R. M. Laine, "Transition Metal Carbides and Process for Making Same," U.S. Pat. No. 4 789 534, Dec. 1988. (b) R. M. Laine, "Method of Preparing Metal Carbides and the Like and Precursors Used in Such Method," U.S. Pat. No. 4 826 666, May 1989. (c) R. M. Laine, "Method of Preparing Coatings of Metal Carbides and the Like," U.S. Pat. No. 4 906 493, March 1990.

[22](a) J. N. Musher and R. G. Gordon, "Atmospheric Pressure Chemical Vapor Deposition of TiN from Tetrakis (dimethylamido) Titanium and Ammonia," *J. Mater. Res.*, **11** [4] 989–1001 (1996). (b) Z. Duan and J. G. Verkade, "Synthesis and Characterization of a Novel Azatitanatrane," *Inorg. Chem.*, **34** [8] 4311–16 (1995). (c) M. E. Gross and T. Siegrist, "Molecular Precursor Chemistry for TiN: Synthesis and Structure of $[Ti(NMe_2)(N_3)(\mu\text{-}NMe_2)]_3(\mu_3\text{-}N_3)(\mu_3\text{-}NH)$," *Inorg. Chem.*, **31** [11] 4898–99 (1992).

[23]Y. W. Bae, W. Y. Lee, C. S. Yust, P. J. Blau, and T. M. Besmann, "Synthesis and Friction Behavior of Chemically Vapor Deposited Composite Coatings Containing Discrete TiN and MoS_2 Phases," *J. Am. Ceram. Soc.*, **79** [4] 819–24 (1996).

[24]R. M. Laine and A. S. Hirschon, "The Pyrolytic Transformation of Organometallic Compounds into Refractory Metals: Tungsten and Molybdenum Carbides"; pp. 21–31 in *Transformation of Organometallic into Common and Exotic Materials: Design and Activation*. Edited by R. M. Laine. Martinus Nijhoff, Dordrecht, The Netherlands, 1988.

[25]G. M. Brown and L. Maya, "Ammonolysis Products of the Dialkylamides of Titanium, Zirconium, and Niobium as Precursors to Metal Nitrides," *J. Am. Ceram. Soc.*, **71** [1] 78–82 (1988).

[26]J. Hapke and G. Ziegler, "Synthesis and Pyrolysis of Liquid Organometallic Precursors for Advanced Si-Ti-C-N Composites," *Adv. Mater.*, **7** [4] 380–84 (1995).

[27](a) Z.-F. Zhang, R. A. Kennish, K. A. Blohowiak, M. L. Hoppe, and R. M. Laine, "Superconducting Fibers From Organometallic Precursors. Part III, High-Temperature Pyrolytic Processing," *J. Mater. Res.*, **8**, 1777–90 (1993). (b) Y. Liu, Z.-F. Zhang, B. King, J. Halloran, and R. M. Laine, "Synthesis of Yttrium Aluminum Garnet from Yttrium and Aluminum Isobutyrate Precursors," *J. Am. Ceram. Soc.*, **79** [2] 385–94 (1996).

[28]K. A. Youngdahl, R. M. Laine, R. A. Kennish, T. R. Cronin, and G. A. Balavoine, "New Catalytic Routes to Preceramic Polymers: Ceramic Precursors to Silicon Nitride and Silicon-Carbide Nitride"; pp. 489–95 in Materials Research Society Symposium Proceedings, Vol. 121, *Better Ceramics Through Chemistry III*. Edited by C. J. Brinker, D. E. Clark, and D. R. Ulrich. Materials Research Society, Pittsburgh, PA, 1988.

[29]L. Maya, D. R. Cole, and E. W. Hagaman, "Carbon–Nitrogen Pyrolyzates: Attempted Preparation of Carbon Nitride," *J. Am. Ceram. Soc.*, **74** [7] 1686–88 (1991).

[30]K. Ogata, "Properties of Carbon Nitride Films with Composition Ratio C/N = 0.5–3.0 Prepared by the Ion and Vapor Deposition Method," *J. Appl. Phys.*, **76** [6] 3791–96 (1994).

[31]J. Jagielski, N. Moncoffre, G. Marest, and S. Fayeulle, "Migration of Nitrogen Implanted into Iron Induced by the Presence of a Buried Carbon-Rich Layer," *J. Appl. Phys.*, **76** [9] 5132–35 (1994).

[32]O. Matsumoto, T. Kotaki, H. Shikano, K. Takemura, and S. Tanaka, "Synthesis of Carbon Nitride in Plasma Arc," *J. Electrochem. Soc.*, **141** [2] L16–L18 (1994).

[33]S. P. Withrow, J. M. Williams, S. Prawer, and D. Barbara, "New Carbon Nitride Phase by High-Dose N Ion Implantation in Glassy Carbon," *J. Appl. Phys.*, **78** [5] 3060–65 (1995).

[34]R. P. Subrayan and P. G. Rasmussen, "An Overview of Materials Composed of Carbon and Nitrogen," *Trends Polym. Sci. (Cambridge, UK)*, **3** [5] 165–72 (1995).

[35](a) J. S. Colligon, H. Kheyrandish, L. N. Lesnevsky, A. Naumkin, A. Rogozin, I. I. Shkarban, L. Vasilyev, and V. E. Yurasova, "Composition and Chemical State of Titanium Nitride Films Obtained by Different Methods," *Surf. Coat. Technol.*, **70** [1] 9–17 (1994). (b) C. D. Wagner, W. M. Riggs, L. E. Davis, and J. F. Moulder, *Handbook of X-Ray Photoelectron Spectroscopy*. Edited by G. E. Muilenberg. Perkin-Elmer, Norwalk, CT, 1979.

[36]Y. Liu and R. M. Laine; unpublished results. □